Synthesis and spark plasma sintering of sub-micron HfB2

Venugopal, S.; Paul, A.; Vaidhyanathan, B.; Binner, Jonathan; Heaton, A.; Brown, P. M.

DOI:
10.1016/j.jeurceramsoc.2013.12.025

Document Version
Peer reviewed version

Citation for published version (Harvard):
Venugopal, S, Paul, A, Vaidhyanathan, B, Binner, J, Heaton, A & Brown, PM 2014, 'Synthesis and spark plasma sintering of sub-micron HfB_2: effect of various carbon sources', *Journal of the European Ceramic Society*, vol. 34, no. 6, pp. 1471-1479. https://doi.org/10.1016/j.jeurceramsoc.2013.12.025

Synthesis and Spark Plasma Sintering of Sub-Micron HfB_2: Effect of Various Carbon sources

Venugopal S[ai], Paul A[a], Vaidhyanathan B[a], Binner JGP[a], Brown PM[b].

[a]Department of Materials, Loughborough University, UK, LE11 3TU

[b]DSTL, Porton Down, Salisbury, UK, SP4 0JQ

Abstract

The difficulties associated with the densification of HfB_2 are well known due to the material's high strength covalent bonding, low self-diffusion coefficient, the presence of oxygen impurities and the fact that the commercially available HfB_2 powders generally have coarse particle sizes of around 1 – 2 μm with consequent poor sinterability. Since it is known that the sinterability of ceramics increases with a decrease in the particles size [1] and there is a growing demand to make complex, dense shapes using HfB_2 powder, there is a need to synthesise fine HfB_2 powders with carefully controlled levels of agglomeration [2]. The present work describes a simple process to synthesise HfB_2 powder with sub-micron sized particles. Hafnium chloride and boric acid were used as the elemental sources whilst several carbon sources including sucrose, graphite, carbon black, carbon nanotubes and liquid and powder phenolic resin were used. The carbon sources were characterized using thermogravimetric analysis and transmission electron microscope. The effect of the structure of the carbon source used, on the size and morphology of the resultant HfB_2 powder was studied; the HfB_2 powders were characterized using X-Ray diffraction and scanning and transmission electron microscopy. The powder synthesized using powder phenolic resin had a surface area of 21 m^2 g^{-1} and a

[i] Corresponding author at: Department of Materials, Loughborough University, Loughborough, Leicestershire LE11 3TU, UK. Tel.: +44 1509223168; fax: +44 1509223949. E-mail address: S.Venugopal@lboro.ac.uk (S. Venugopal).

particle size distribution between 30 – 150 nm. It also contained less agglomeration than the powders resulting from other precursors. This was sintered using SPS to a theoretical density of 94% at 2100^{o}C and 50 MPa pressure without the help of any sintering aids.

Keywords: Ultra-high temperature ceramics, HfB_2, carbon sources, nano particles, SPS, sintering

1. Introduction

Hafnium diboride (HfB_2) is a potential material for high-temperature structural applications due to its high melting temperature, high strength, and high thermal and electrical conductivity [3]. Its strong covalent bonding and low self-diffusion however, means that either very high temperatures and/or high pressures are required to densify it [3,4]. Both reactive hot pressing [5,6] and spark plasma sintering [7] have been used typically with additives such as carbon, B_4C [8], WC, or silicides (Si_3N_4, $HfSi_2$, $TaSi_2$, $TiSi_2$ and $MoSi_2$ [9]). These form a liquid phase and hence reduce the sintering temperature, however the resulting glassy grain boundary phases often reduce the high temperature strength and mechanical properties [10]. In addition, to achieve a homogeneous diboride-additive mixture extensive milling is typically used which, in turn, introduces impurities further decreasing the high temperature performance [11]. This work focuses on the preparation of hafnium diboride powders with fine particle size, high purity and low levels of agglomeration. Most commercially available powders have an average particle size of 1 μm and hence demonstrate poor sinterability.

A large number of routes have been reported to synthesize HfB_2 powder, as shown in Table 1. The most widely used is boro/carbothermal synthesis where an oxide or halide precursor of Hf is reduced using a suitable carbon and boron source.

Table 1: Literature data on synthesis routes for HfB_2

Synthesis Route	Precursors	Heat treatment conditions	Particle sizes yielded	References
Boro/carbothermal reduction	HfO_2, B_4C, C	1600°C, 1650°C, 1875°C, 1 – 2 h	0.25 – 2 µm	[4, 12, 13, 14, 16]
Borothermal reduction	HfO_2, amorphous B	1550°C, 1 h	0.8 µm	[15]
Mechanically activated synthesis	$HfCl_4$, B, Mg	1100°C	1 µm	[16]
Pressure activated synthesis	$HfCl_4$, $NaBH_4$	600°C, 12 h	25 nm	[17]
Non-self propagating high temperature synthesis	Hf sheet, amorphous B, carbon black	1500°C	-	[18]

SPS has been used for fabricating dense HfB_2–SiC [19], TiB_2–WB_2–CrB_2 [20], HfB_2–$MoSi_2$ [21], and HfC and HfB_2-based composites with $MoSi_2$ additives [22, 23]; however a dense HfB_2 without any sintering aid is yet to be achieved.

In the current work the effect of different carbon sources with different structures, on the size and morphology of the synthesized HfB_2 powder particles is reported. Hafnium chloride ($HfCl_4$) and boric acid (H_3BO_3) were used as the sources of Hf and B respectively. The carbon sources included liquid and powder phenolic resin, pitch, sucrose, graphite, carbon black and carbon nanotubes. The operational mechanism by which the carbon sources affected the particle size has been determined and the XRD phase pure sub micron-sized HfB_2 powder has been synthesized. A comparison between the sinter-ability of a commercially procured HfB_2 and the fine HfB_2 synthesized in the present work using SPS densification is also presented.

2. Experimental

Table 2 provides a list of the different starting materials used and their suppliers. The carbon content of each carbon source was obtained from thermo gravimetric analysis (Q5000IR TGA, TA instruments, Zellik, Belgium). The samples were heated up to 1000^{o}C in an Ar atmosphere using a heating rate of 5^{o}C min^{-1} and the weight loss curves obtained. In order to study the structure of the carbon resulting from the pyrolysis of the different carbon sources, the latter were dissolved in ethanol (water for sucrose) and refluxed at 120^{o}C for 24 h with subsequent drying and grinding. The product was then heated to 1000^{o}C in an argon atmosphere in a high temperature horizontal tube furnace (TSH17/75/450, Elite Thermal Systems Ltd, UK) fitted with a 99.7% pure alumina tube. The heating and cooling rates were maintained as 5^{o}C min^{-1}.

The synthesis approach used was similar to a process described previously [14]. A carbon source, dissolved and/or suspended in ethanol [ii], was added to a boric acid/ethanol solution held at 120^{o}C. $HfCl_4$ that had been dissolved in ethanol was then added and the mixture was allowed to stir for 24 hours at 120^{o}C under reflux conditions. This was followed by subsequent drying in an oven at 250^{o}C for 2 hours and grinding using a mortar and pestle to get the HfB_2 precursor powders.

[ii] Being immiscible in ethanol, the sucrose was dissolved in water and hence the $HfCl_4$ and boric acid were also dissolved in water.

Table 2: Raw materials used in this study

Chemical/Raw materials	Molecular formula	Source	Purity / Carbon content @ 1000°C
Hafnium chloride	$HfCl_4$	Sigma Aldrich, Dorset, UK	98% purity
Boric acid	H_3BO_3	Fischer Scientific, Loughborough, UK	99.5% purity
Liquid phenolic resin (LPR)	$[(HOC_6H_4)_2CH_2]_n$	Cellobond J2027L, Momentive Speciality Chemicals, Louisville, USA	51% carbon content
Powder phenolic resin (PPR)	$[(HOC_6H_4)_2CH_2]_n$	Crios resins, SI group, Inc, S□o Paulo, Brazil	41.7% carbon content
Sucrose	$C_{12}H_{22}O_{11}$	Fischer Scientific, Loughborough, UK	21.8% carbon content
Pitch	Carbores® P	Rutgers chemicals, Zelzate, Belgium	65.6% carbon content
Graphite	C; 325 mesh	Fischer Scientific, Loughborough, UK	99% purity
Multi walled carbon nano tube (MWCNT)	C; 10 – 20 nm diameter	NTP, Shenzhen, China	>97% purity
Carbon black N115	C; 20 – 40 nm, oil absorption co-efficient* 1.1 ml/g	Columbian Chemicals UK, Bristol, UK	>99% purity
Carbon black N772	C; 100 – 150 nm, oil absorption co-efficient* 0.65 ml g^{-1}	Columbian Chemicals UK, Bristol, UK	>99% purity
Absolute Ethanol	C_2H_5OH	Fischer Scientific, Loughborough, UK	99.9% purity

*Oil absorption co-efficient: a measure of the structure i.e. degree of aggregation/agglomeration present in the carbon black powder [24].

The HfB_2 precursor powders synthesized were subjected to boro/carbothermal reduction (BCTR) in the same horizontal tube furnace (TSH17/75/450, Elite Thermal Systems Ltd, UK). The heating and cooling rates were maintained at $5^oC\ min^{-1}$ up to 1000^oC and $3^oC\ min^{-1}$ above 1000^oC and a flowing argon atmosphere was used throughout. The BCTR synthesis temperature used in this study was 1600^oC for 2 h. An estimation of the particle size of the powders was obtained using field emission electron microscopy (FEGSEM 1530 VP, Carl Zeiss (Leo), Oberkochen, Germany) and transmission electron microscopy (TEM 100 CX, JEOL JEM, Munich, Germany). Phase analysis was performed by XRD (Bruker D8 X-Ray Diffractometer, Bruker, Coventry, UK) using Cu Kα radiation. The d spacings were calculated from the 2θ values and were compared with the standard values from the JCPDS powder diffraction files to identify the phases. The particle size distribution was obtained using a Mastersizer 2000 (Malvern, Worchestershire, UK) using prop-3-ol (99%, Fisher Scientific, Loughborough, UK) as the solvent. The BET surface area was analysed using a gas adsorption analyser (Micrometrics TriStar 3000, Norcross, USA).

The finest of all the synthesized HfB_2 powders achieved was sintered using spark plasma sintering (SPS) in vacuum at 1900, 2000 and 2100^oC for 10 min. 10 grams of the powder was cold pressed at 62 MPa pressure and placed in graphite foil-lined, 20 mm diameter graphite dies, the latter being covered with graphite felt to reduce heat loss. A load of 50 MPa was applied from 1000^oC and was maintained thorough the sintering and cooling step. The heating rate and the cooling rates were $100°C\ min^{-1}$ and $50°C\ min^{-1}$ respectively. The linear change in shrinkage was recorded during sintering by monitoring the displacement of the sample along the pressing direction. It should be noted that the optical pyrometer was focused on the surface of the graphite die and not directly on the specimen, which will have given rise to a difference between the temperature of the die and that of the specimen, especially at the faster heating rates and shorter hold times. Similar runs were carried out for 99% pure HfB_2 powder with d_{50}

= 2 µm procured from Treibacher, Austria. The density of the sample was measured using the Archimedes principle, using the theoretical density as 11.1 g/ cm^{-3} [25], and the grain size was studied by imaging their surfaces using Solid state retractable backscatter detector with low voltage capability (Nova 600 Nanolab Dual Beam, Eindhoven, The Netherlands).

3. Results and Discussion

i. Synthesis and effect of carbon sources

The thermogravimetric analysis of the carbon sources, excluding graphite, carbon nanotubes and carbon black since they have no volatiles, is shown in Figure 1. All of the carbon sources tested showed an initial weight loss curve that plateaued as the temperature increased over 600^{o}C. The weight loss was highest for sucrose with a residual carbon content of just 21.8%; pitch had the lowest weight loss with a residual mass of 65.6%. The sucrose was stable up to 200^{o}C after which there was a very significant weight loss caused by dehydration, dehydrogenation and volatilization of CO and CO_2 [26]. The pitch showed no mass loss up to 350^{o}C due to the absence of both physically and chemically bonded water, after which it slowly began to lose weight due to breaking of the aromatic chains and dehyrdrogenative cross linking during the process of pyrolysis [27]. The liquid and powder phenolic resins lost water until they cured at around 145^{o}C. Beyond this temperature the weight loss remained almost stable up to 400^{o}C and only CO and CO_2 degassing occurred. The degradation of the resin then started, involving the release of volatile compounds like phenol, cresol, and toluene [28]. The residual weight of each carbon source after pyrolysis in argon, which was the weight of the carbon present in the chemical, was obtained and used for further calculations.

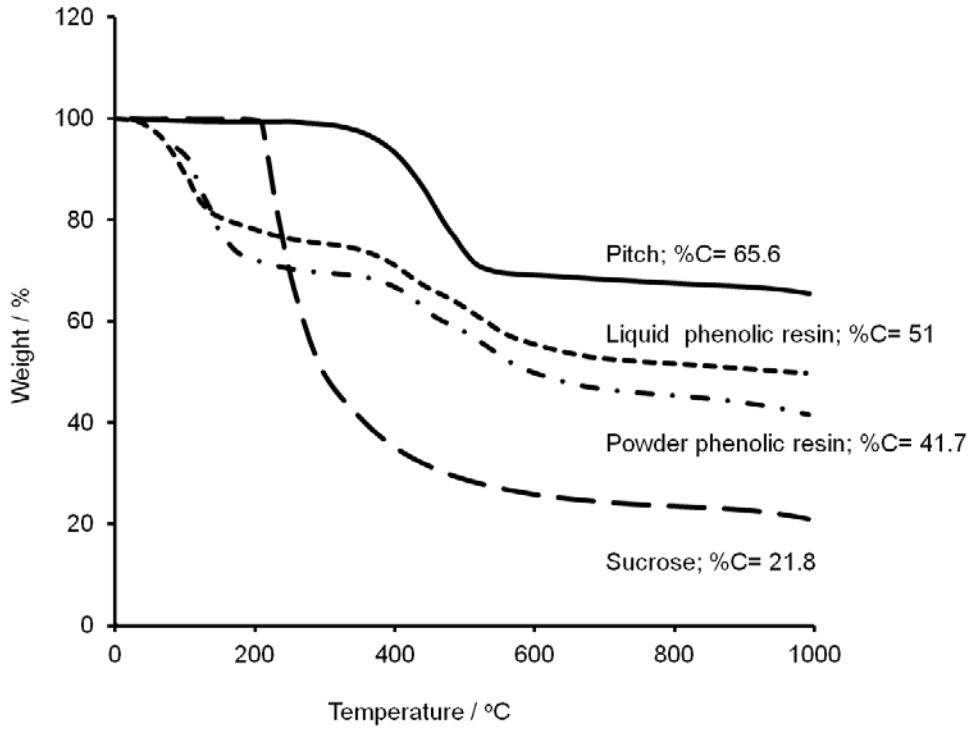

Figure 1: TGA of carbon sources

In every case the final powders obtained by heat treating the hafnium and boron precursors with the different carbon sources at 1600^{o}C for 2 h was single phase hexagonal hafnium diboride; the XRD result for one system is shown in Figure 2.

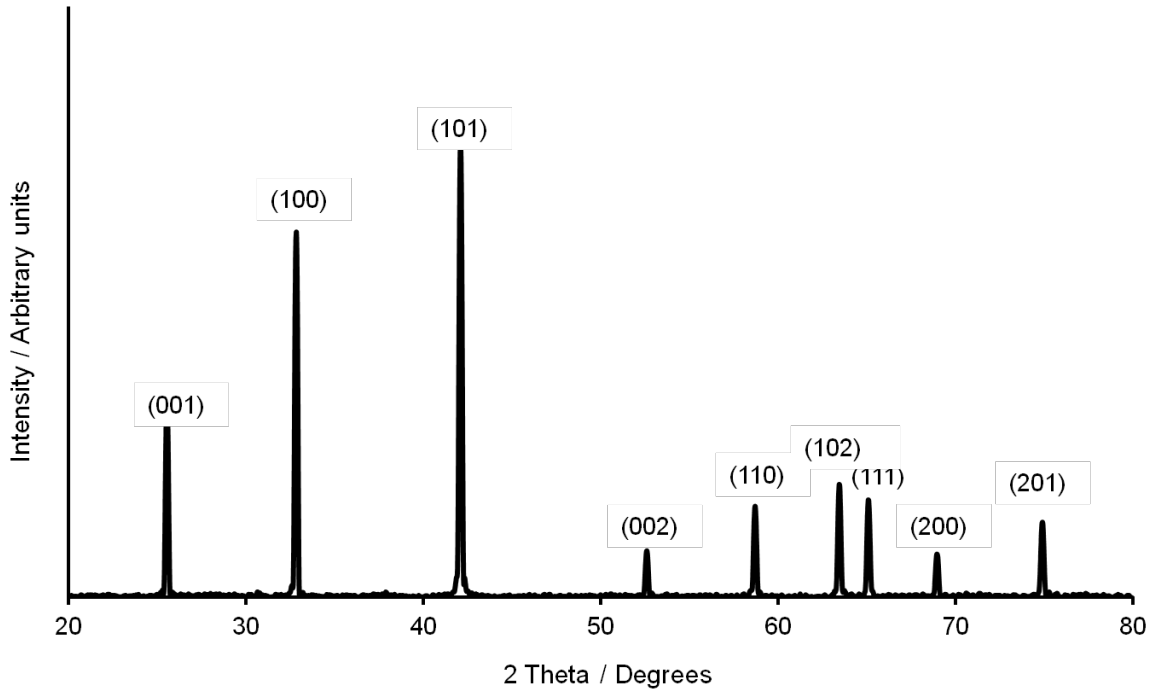

Figure 2: XRD of the HfB_2 powder prepared using Hf, B and LPR after heat treatment at 1600^{o}C for 2 h

The peaks are indexed according to JCPDS 00-038-1398. Figure 3, shows the TEM images (on the left) of the different carbon sources after pyrolysis and FEGSEM images (on the right) of the corresponding HfB_2 powders synthesized from these sources. Since the only difference between the different precursor powders was the carbon source, the differences in the size and/or structure of the particles in the final powders can be attributed to the carbon source used. The carbon from pitch was spherical and very uniform and so was the final HfB_2 powder produced, Figure 3a; the particle size was approximately 1.5 µm. Sucrose and graphite both form sheet-like carbon and the HfB_2 particle sizes obtained from them were around 1 µm and 3 µm respectively, Figure 3b and c. The effect of the carbon being in the form of sheets will be discussed shortly.

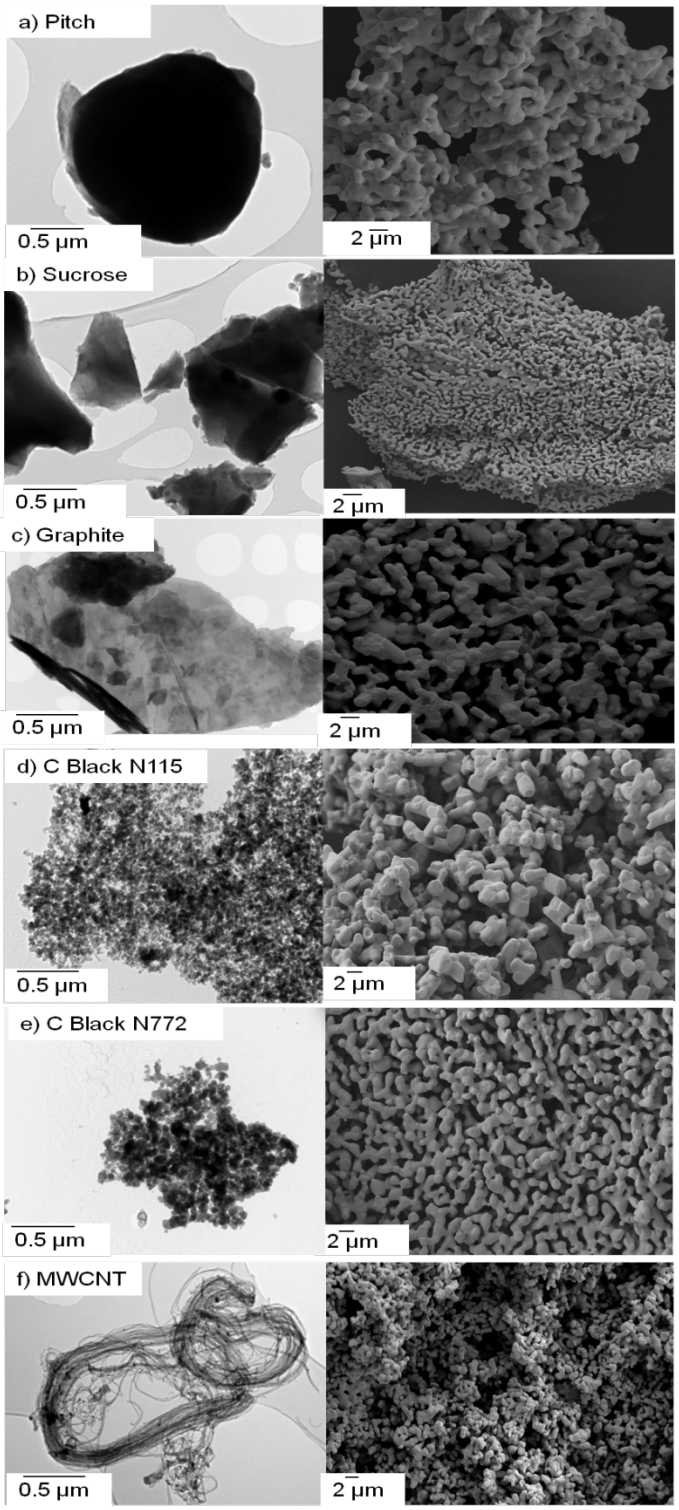

Figure 3: TEM images of the carbon structures (left) resulting from the pyrolysis of different carbon sources at 1000^{o}C for 0.1 h and the corresponding FEGSEM images of the resultant HfB_2 powders after heat treatment at 1600^{o}C for 2 h using a) pitch, b) sucrose, c) graphite, d) C-Black N115, e) C-Black N772 and f) MWCNT

For the HfB_2 powders resulting from the carbon black and multi-walled carbon nano tubes, Figures 3d – f, the final particle size was influenced by the level of agglomeration of the pyrolysed carbon sources. For instance, carbon black N115 had much finer particles at ~20 nm than carbon black N772 at ~150 nm, but the structure factor was higher for the former, meaning that it was more heavily agglomerated. This led to the resultant HfB_2 particles actually being coarser when made from N115. The average particle size of HfB_2 powders obtained from these sources was between 1 – 3 µm. Similarly, although the diameter of the MWCNT were only 10 – 20 nm, the tubes were heavily entangled and the resulting HfB_2 particles were 0.8 – 1 µm in size.

Figure 4 shows the electron micrographs of the carbon structures resulting from heat treating the liquid phenolic resin (LPR) to 1000^{o}C for 0.1 h and the resulting HfB_2 powder. The carbon resulting from LPR was in the form of a sheet as for the sucrose and graphite, and the size and the level of agglomeration of the sheets directly influenced the size of the HfB_2 particles in the final product formed as illustrated in Figure 5.

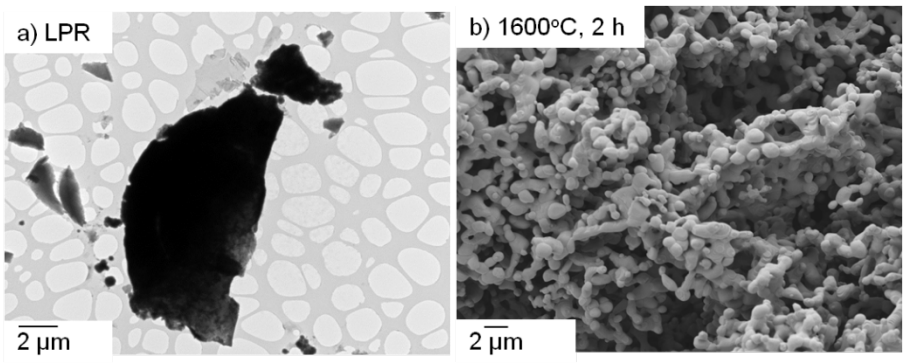

Figure 4: a) TEM image of the carbon structure resulting from pyrolysis at 1000^{o}C for 0.1 h and b) a FEGSEM image of the resultant HfB_2 powder

It is believed that the sheet-like carbon resulting from the LPR acted like a matrix with the Hf and B precursors being embedded in it. Figure 5a, shows the structure after heating to 1000^{o}C

for 0.1 h; several islands of the carbon sheets may be seen with the embedded ceramic particles appearing clearly within them. The different situations are illustrated in Figure 5b, c, d and e, one with excess carbon and one with the stoichiometric carbon content. If excess carbon was present then the carbon matrix prevented the ceramic particles from coalescing and growing larger, resulting in fine HfB_2 particles of 20 – 80 nm, Figure 5b, but retaining a significant carbon impurity. On the other hand, if the stoichiometric amount of carbon was present then the matrix was consumed in the process of HfB_2 formation and the ceramic particles tended to coalesce, becoming 1 – 3 µm in size, Figure 5d and e. It is believed that this explanation is also valid for other carbon sources, sucrose and graphite, where pyrolysis yielded sheet-like carbon.

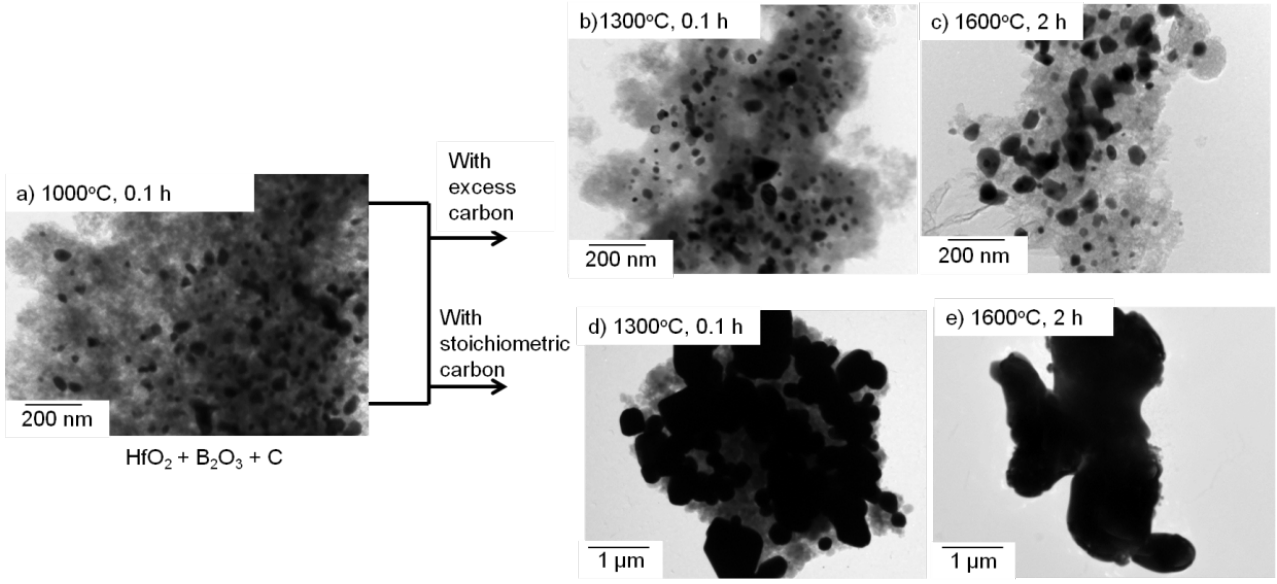

Figure 5: Method of formation of HfB_2 powder with LPR as the carbon source

The finest HfB_2 was obtained when using the powder phenolic resin (PPR) as the carbon source. The latter yielded tiny, well dispersed particles of carbon on pyrolysis, Figure 6a-e and consequently the resultant HfB_2 particles were 30 – 150 nm in size. Figure 6c shows the formation of the HfB_2 particles as a result of different calcination temperatures.

At 700^{o}C the ceramic particles and the carbon from the PPR were well dispersed and intermixed, with the carbon forming tail-like structures for the ceramic particles. As the calcination temperature increased the carbon appeared to prevent much growth of the ceramic particles in a similar manner to LPR but on a finer scale. After heat treatment at 1600^{o}C for 2 h the carbon was consumed and each ceramic particle grew at the expense of its neighbours, yielding HfB_2 particles of the approximate shape and size of the carbon island in which it was contained.

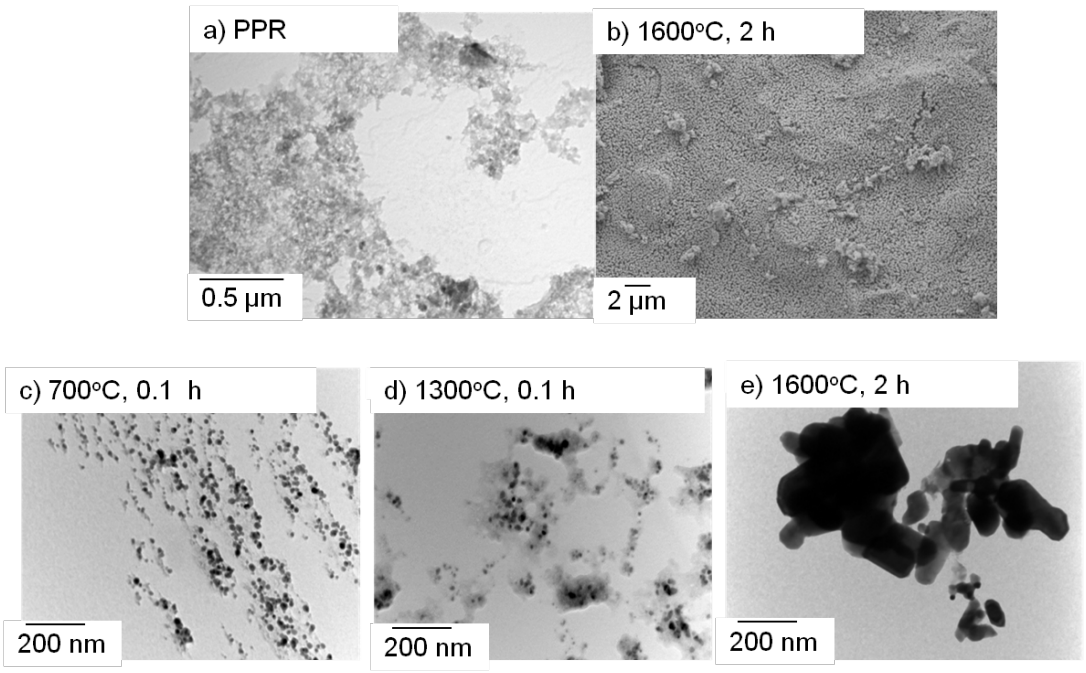

Figure 6: a) TEM image of carbon structure resulting from heat treating PPR to 1000^{o}C for 0.1 h, b) FEGSEM picture of HfB_2 powders made using PPR and c, d, e) formation of HfB_2 powder from PPR

Figure 7 shows the particle size analysis of the HfB_2 powder formed from the PPR carbon source as measured using the Malvern mastersizer. The d_{10}, d_{50} and d_{90} number % values were 30, 70 and 130 nm respectively, whilst the volume % values were 90, 200, 2331 nm respectively; the BET surface area was 21.8 m^2 g^{-1}. The particle size obtained from the BET surface area value was 26 nm. The volume % shows very little agglomeration in the sample.

Table 3 summarises the carbon sources used and the size of the resultant powders produced.

Table 3: Carbon sources used and the size of the resultant HfB_2 powders

Carbon source	**HfB_2 particle size / µm**
Liquid phenolic resin	0.5 – 2
Pitch	1.5 – 2
Sucrose	1 – 2
Graphite	3 – 4
Carbon black N 772	1 – 2
Carbon black N 115	2 – 3
Multi walled carbon nano tube	0.8 – 1
Powder phenolic resin	0.03 – 0.15

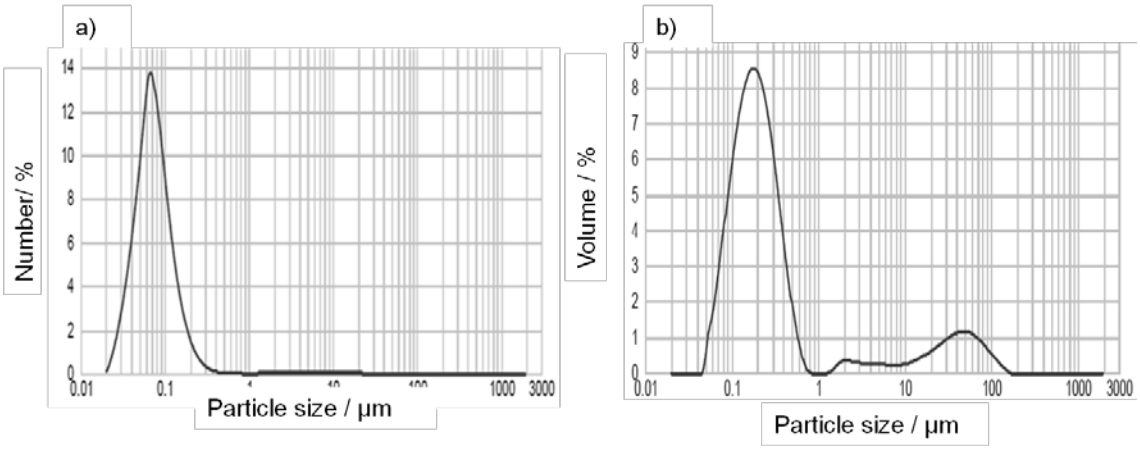

Figure 7: Particle size analysis for the HfB_2 powder synthesized using PPR as the carbon source and calcined at 1600^{o}C for 2 h a) Number %, b) Volume %

ii) Sintering

The fine HfB_2 powder obtained when using PPR as the carbon source and the commercial powders obtained from Treibacher, Germany (fine grade) were sintered at different temperatures using spark plasma sintering as outlined in the experimental section. The time, temperature and force profiles are given in Figure 8. The pressure was kept as a constant at 16 kN in all the cases. The time-displacement curves at 1900^{o}C, 2000^{o}C and 2100^{o}C for the commercial and LU powders is given in Figure 9. The densification of both the commercial and LU HfB_2 appeared to start around 1400^{o}C in all the cases. However, the percentage densification of LU powder seemed to overtake the commercial powder with every 100^{o}C rise in temperature, due to its higher surface area leading to more shrinkage.

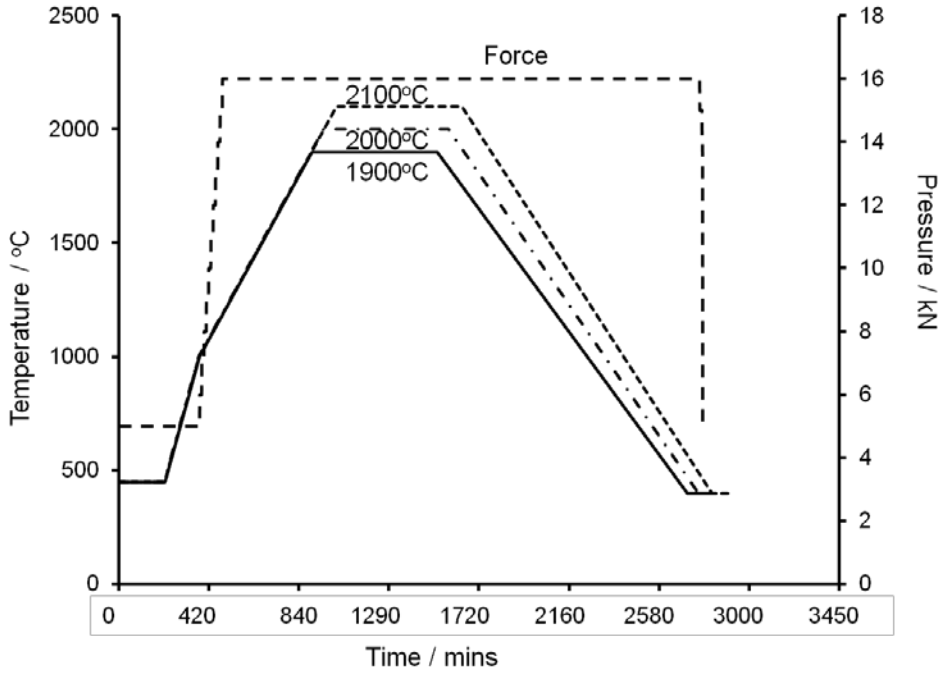

Figure 8: Time temperature force profile used for SPS of the fine HfB_2 powders

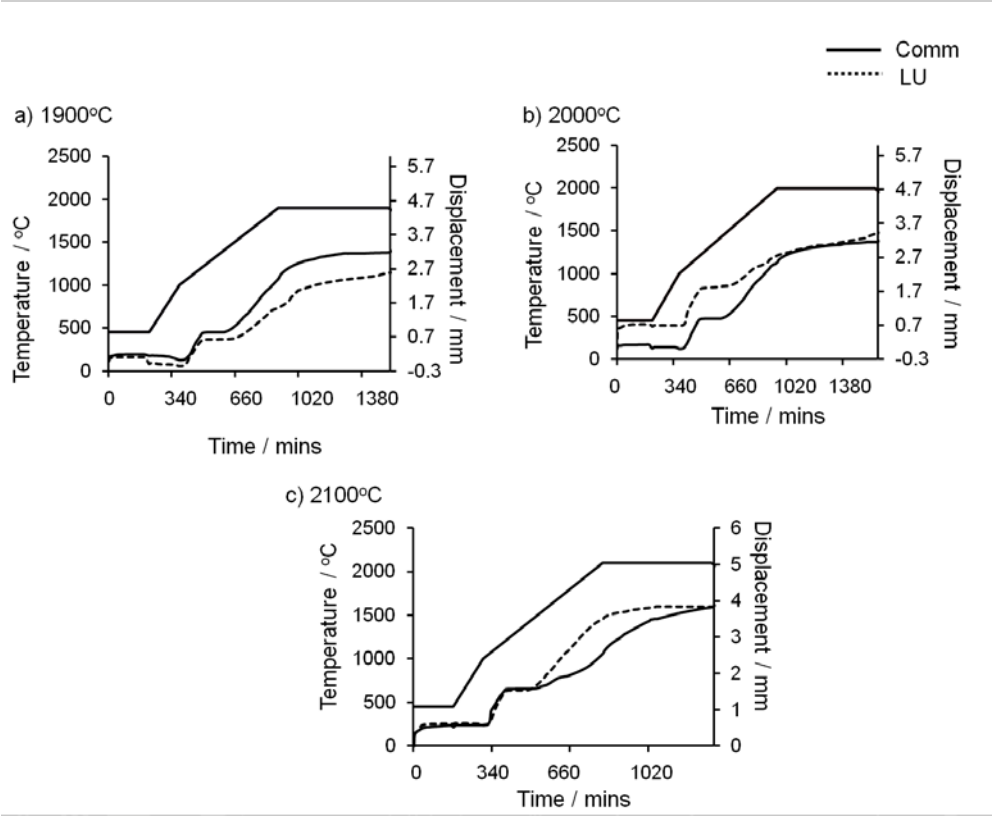

Figure 9: Time evolution of SPS parameters during densification at a) 1900°C, b) 2000°C and c) 2100°C

Figure 10a-c shows the FEGSEM images of the Treibacher powders (left) and Loughborough (LU) synthesized fine powders (right) sintered at 1900^{o}C, 2000^{o}C, and 2100^{o}C for 10 mins, along with their theoretical density values. As seen from the images, the LU HfB_2 powders have a finer grain size, which is indicative of the fine size of the starting powder. The density of the commercial samples did not increase with the increase in temperature, however, the grain size did increase, trapping pores within the grains. For the sample sintered at 2100^{o}C and 50 MPa pressure, the grain size ranged between 20 – 40 μm and the theoretical density was 93%. On the other hand, the density along with the grain size of the LU HfB_2 increased linearly with the increase in temperature, reaching a maximum theoretical density of 94% and a grain size of 1 – 2 μm at 2100^{o}C and 50 MPa pressure. With its covalent bonding and low self-diffusion co-efficient, HfB_2 is difficult to sinter without any addition of sintering aids, however the nanometer sized powder sintered to 94% of theoretical density at 2100^{o}C whilst retaining a fine grain size. Sciti et al. [29] obtained monolithic HfB_2 ceramics with relative density of ~ 80.0% by SPS at 2200^{o}C and 95 MPa pressure using commercially available powders. The smallest grain size and highest density ever achieved was through reactive SPS at 1700^{o}C and 95 MPa. A 98% dense and ≈10 μm wide grains was attributed to the absence of surface oxidation in this single step synthesis and sintering [30].

In order to further improve the density of the monolith sintered bodies, the pressure applied during SPS could be increased up to 200 MPa, or reactive SPS similar to the approach used by Munir et.al [30] could be exploited.

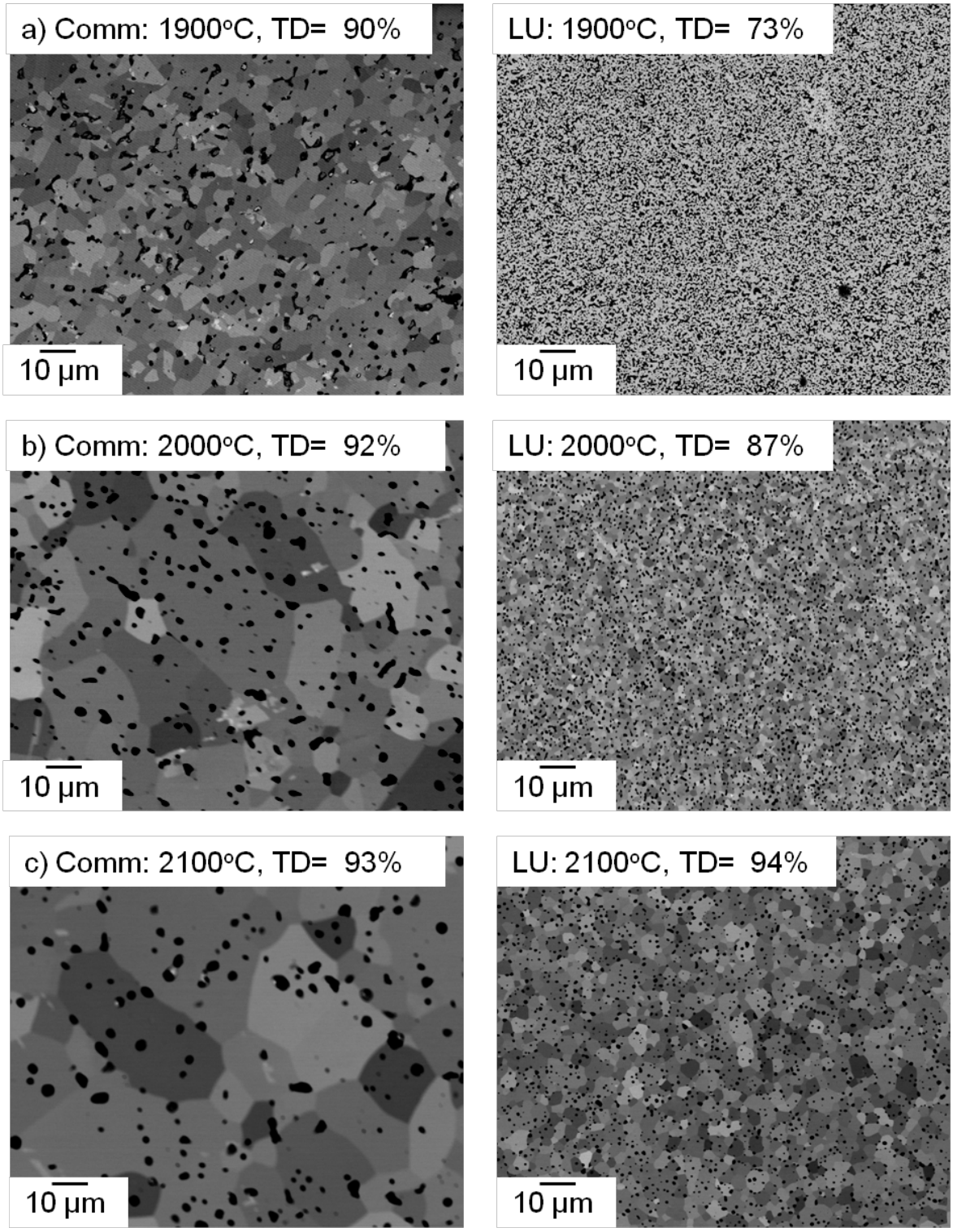

Figure 10: BS images of the polished surface of commercial (left) and LU fine (right) HfB_2 powders spark plasma sintered at a) 1900°C, b) 2000°C and c) 2100°C for 10 min under 50 MPa pressure

4. Conclusion

HfB_2 powders were synthesized at 1600^oC for 2 h using various carbon sources like LPR, pitch, sucrose, graphite, carbon black, carbon nanotubes and PPR. It was found that the structure and the level of agglomeration of the carbon source had a direct influence on the particle size of HfB_2 powder. LPR, sucrose, graphite, and PPR on pyrolysis resulted in a sheet like carbon that engulfed the ceramic particles. Tiny and well dispersed sheets resulted in finer and agglomeration free HfB_2 particles. For carbon black and carbon nanotubes the size of the resultant HfB_2 particles was directly dependent on the level of agglomeration of carbon sources. The finest HfB_2 powder was obtained when using PPR as the carbon source and the particle size was between 30 – 150 nm and a surface area of 21.8 m^2 g^{-1}. SPS sintering of the sub-micron sized HfB_2 powders obtained using PPR as the carbon source at 2100^oC and 50 MPa resulted in 94% dense body and a grain size of 1 – 2 μm, whilst under the same sintering conditions commercial powders had grain sizes ranging between 20 – 40 μm.

Acknowledgement

The authors would like to thank Dr Salvatore Grasso, Post-Doctoral research assistant at Queen Mary University, London for help with spark plasma sintering of the samples.

Funding from Defence Science and Technology Laboratories (DSTL), UK is acknowledged.

References

[1] P. L. Chen and I. W. Chen, 'Sintering of Fine Oxide Powders: II, Sintering Mechanisms', *J. Am. Ceram. Soc.*, 80 [3] 637– 645 (1997).

[2] F.F. Lange, 'Sinterability of Agglomerated Powders', *J. Am. Ceram. Soc.*, **67** (1984).

[3] W. G. Fahrenholtz and G. E. Hilmas, 'Refractory Diborides of Zirconium and Hafnium', *J. Am. Ceram. Soc.*, 90 [5] 1347–1364 (2007).

[4] G. J Zhang, W. M. Guo, D. W Ni, and Y. M Kan, 'Ultrahigh temperature ceramics (UHTCs) based on ZrB_2 and HfB_2 systems: powder synthesis, densification and mechanical properties', *J. Phy. Conference Series*, 176 (2009).

[5] G. J Zhang, Z. Y. Deng, N. Kondo, J. F.Yang, T. Ohji, 'Reactive Hot Pressing of ZrB_2 – SiC Composites', *J. Am. Ceram. Soc.*, 83 [9] 2330 – 2332 (2000).

[6] W. Wu, G. Zhang, Y. Kan, P. Wang, 'Reactive hot pressing of ZrB_2-SiC-ZrC ultra high-temperature ceramics at 1800^{o}C', *J. Am. Ceram. Soc.*, 89 2967 – 2969 (2006).

[7] A. Paul, S. Venugopal, J. Binner, B. Vaidhyanathan, D. D. Jayaseelan, E. Zapata-Solvas, W. E. Lee, A. Heaton, P. Brown, 'UHTC composites for hypersonic applications', *Am. Ceram. Soc. Bull.*, 91 22-28 (2012).

[8] J. Brown-Shaklee, W. G. Fahrenholtz, and G. E. Hilmas, 'Densification Behavior and Microstructure Evolution of Hot-Pressed HfB_2', *J. Am. Ceram. Soc.*, 94 49–58 (2011).

[9] D. Scitia, G. Bonnefontb, G. Fantozzib, L. Silvestronia, 'Spark plasma sintering of HfB_2 with low additions of silicides of molybdenum and tantalum', *J. Eur. Ceram. Soc.*, 30 3253 – 3258 (2010).

[10] E. Wuchina, M. Opeka, S. Causey, K. Buesking, J. Spain, A. Cull, J. Routbort, F. Guitierrez-Mora, 'Designing for ultrahigh-temperature applications: The mechanical and thermal properties of HfB_2 , HfC_x , HfN_x and Hf(N)', *J. Mater. Sci.*, 39 5939 – 5949 (2004).

[11] D. Sciti, L. Silvestroni, A. Bellosi, 'Fabrication and properties of HfB_2–$MoSi_2$ composites produced by hot pressing and spark plasma sintering', *J. Mater. Res.*, 21 1460-1466 (2006).

[12] D. W. Ni, G. J. Zhang, Y. M. Kan, P. L. Wang, 'Synthesis of Monodispersed Fine Hafnium Diboride Powders using Boro/carbothermal Reduction of Hafnium Dioxide', *J. Am. Ceram. Soc.*, 91 2709 – 2712 (2008).

[13] J. K. Sonbera, T. S. R. Ch. Murthya, C. Subramaniana, S. Kumarb, R. K. Fotedara, A. K. Suri, Investigations on synthesis of HfB_2 and development of a new composite with $TiSi_2$, *Inter. J. Refract. Met. H.* 28, 201 – 210, (2010).

[14] S. Venugopal, E. E. Boakye, A. Paul, K. Keller, P. Mogilevsky, B. Vaidhyanathan, J. G. P. Binner, A. Katz, PM. Brown, Sol Gel Synthesis and Formation Mechanism of Ultra High Temperature Ceramic: HfB_2, *J. Am. Ceram. Soc*., accepted Sep 2013.

[15] W. M. Guo, Z. G. Yang, G. J. Zhang, 'Synthesis of submicrometer HfB_2 powder and its densification', *Mater Lett*, 83 52 – 55 (2012).

[16] S. Bégin-Colin, G. Le Caër, E. Barraud and O. Humbert, 'Mechanically activated synthesis of ultrafine rods of HfB_2 and milling induced phase transformation of monocrystalline anatase particles', *J. Mater. Sci.*, 39 [16–17] 5081–5089 (2004).

[17] L. Chen, Y. Gu, L. Shi, Z. Yang, J. Ma, Y. Qian, 'Synthesis and oxidation of nanocrystalline HfB_2', *J. Alloy. Compd*., 368 353 – 356 (2004).

[18] Y. D. Blum, J. Marschall, D. Hui, B. Adair, and M. Vestel , 'Hafnium Reactivity with Boron and Carbon Sources Under Non-Self-Propagating High-Temperature Synthesis Conditions', *J. Am. Ceram. Soc.*, **91** [5] 1481–1488 (2008).

[19] F. Monteverde, C. Melandri, S. Guicciardi, 'Microstructure and mechanical properties of an HfB_2+30 vol.% SiC composite consolidated by spark plasma sintering', *Mater. Chem. Phy.*, 100 [2-3] 513-519 (2006).

[20] H. Kaga, E. Heian, Z. A. Munir, C. Schmalzried, R. Telle, 'Synthesis of hard materials by field activation: the synthesis of solid solutions and composites in the TiB_2-WB_2-CrB_2 system', *J. Am. Ceram. Soc.*, 84[12] 2764-2770 (2001).

[21] D. Sciti, L. Silvestroni, A. Bellosi, 'Fabrication and properties of HfB_2-$MoSi_2$ composites produced by hot pressing and spark plasma sintering', *J. Mater. Res.*, 21[6] 1460-1466 (2006).

[22] D. Sciti, L. Silvestroni, M. Nygren, 'Spark plasma sintering of Zr- and Hf-borides with decreasing amounts of $MoSi_2$ as sintering aid', *J. Euro. Ceram. Soc.*, 28[6] 1287-1296 (2008).

[23] D. Sciti, S. Guicciardi, M. Nygren, 'Densification and mechanical behavior of HfC and HfB_2 fabricated by spark plasma sintering', *J. Am. Ceram. Soc.*, 91[5] 1433-1440 (2008).

[24] A. J. George, M. H. William, W.M. Ricky, 'Advances in structure measurements of carbon black', *Rubber world*, (2009).

[25] http://www.azom.com/article.aspx?ArticleID=2293

[26] R. Kumaresan, S. Moorthy Babu, 'Crystal growth and characterization of sucrose single crystals', *Mater. Chem. Phy.*, 49 83 – 86 (1997).

[27] S. N. Mashau, 'The preparation of pitches from antracene oil', Master of Science thesis, University of Pretoria, May (2007).

[28] R. Lum, C. W. Wilkins, M. Robbins, A. M. Lyons R. P. Jones, 'Thermal analysis of graphite and carbon-phenolic composites by pyrolysis-mass spectrometry', *Carbon*, 21 111 – 116 (1983).

[29] D. Sciti and S. Guicciardi, 'Densification and Mechanical Behavior of HfC and HfB_2 Fabricated by Spark Plasma Sintering', *J. Am. Ceram. Soc.*, 91 [5] 1433–1440 (2008)

[30] U. Anselmi-tamburini, Y. Kodera, M. Gasch, C. Unuvar, Z. A. Munir, M. Ohyanagi and S. M. JOHNSON, 'Synthesis and characterization of dense ultra-high temperature thermal protection materials produced by field activation through spark plasma sintering (SPS): I. Hafnium Diboride', *J Mater Sci., 41 3097-3104 (2006).*